PHILOSOPHICAL TRANSACTIONS OF THE ROYAL SOCIETY A MATHEMATICAL, PHYSICAL & ENGINEERING SCIENCES

Tipping points in open systems: bifurcation, noise-induced and rate-dependent examples in the climate system

Peter Ashwin, Sebastian Wieczorek, Renato Vitolo and Peter Cox

Phil. Trans. R. Soc. A 2012 **370**, 1166-1184
doi: 10.1098/rsta.2011.0306

PHILOSOPHICAL TRANSACTIONS OF THE ROYAL SOCIETY A

Phil. Trans. R. Soc. A (2012) **370**, 1166–1184
doi:10.1098/rsta.2011.0306

Tipping points in open systems: bifurcation, noise-induced and rate-dependent examples in the climate system

By Peter Ashwin*, Sebastian Wieczorek, Renato Vitolo and Peter Cox

Mathematics Research Institute, University of Exeter, Exeter EX4 4QF, UK

Tipping points associated with bifurcations (B-tipping) or induced by noise (N-tipping) are recognized mechanisms that may potentially lead to sudden climate change. We focus here on a novel class of tipping points, where a sufficiently rapid change to an input or parameter of a system may cause the system to 'tip' or move away from a branch of attractors. Such rate-dependent tipping, or *R-tipping*, need not be associated with either bifurcations or noise. We present an example of all three types of tipping in a simple global energy balance model of the climate system, illustrating the possibility of dangerous rates of change even in the absence of noise and of bifurcations in the underlying quasi-static system.

Keywords: rate-dependent tipping point; bifurcation; climate system

1. Tipping points: not just bifurcations

In the last few years, the idea of 'tipping points' has caught the imagination in climate science with the possibility, also indicated by both palaeoclimate data and global climate models, that the climate system may abruptly 'tip' from one regime to another in a comparatively short time.

This recent interest in tipping points is related to a long-standing question in climate science: to understand whether climate fluctuations and transitions between different 'states' are due to external causes (such as variations in the insolation or orbital parameters of the Earth) or to internal mechanisms (such as oceanic and atmospheric feedbacks acting on different time scales). A famous example is the Milankovich theory, according to which these transitions are forced by an external cause, namely the periodic variations in the Earth's orbital parameters [1]. Remarkably, the evidence in favour of the Milankovich theory still remains controversial [2].

Hasselmann [3] was one of the first to tackle this question through simple climate models obtained as stochastically perturbed dynamical systems. He argued that the climate system can be conceptually divided into a fast component

*Author for correspondence (p.ashwin@ex.ac.uk).

One contribution of 13 to a Theme Issue 'Climate predictions: the influence of nonlinearity and randomness'.

(the 'weather', essentially corresponding to the evolution of the atmosphere) and a slow component (the 'climate', i.e. the ocean, cryosphere, land vegetation, etc.). The 'weather' would act as an essentially random forcing exciting the response of the slow 'climate'. In this way, short-time-scale phenomena, modelled as stochastic perturbations, can be thought of as driving long-term climate variations. This is what we refer to as *noise-induced tipping*.

Sutera [4] studied noise-induced tipping in a simple global energy balance model previously derived by Fraedrich [5]. Sutera's results indicate a characteristic time of 10^5 year for the random transitions between the 'warm' and the 'cold' climate states, which matches well with the observed average value. One shortcoming is that this analysis leaves open the question as to the *periodicity* of such transitions indicated by the power spectral analysis [6, fig. 7].

There is a considerable literature on noise-induced escape from attractors in stochastic models [7]. These have successfully been used for modelling changes in climate phenomena [8], although authors do not always use the word 'tipping' and other aspects have been examined. For example, Kondepudi *et al.* [9] considered the combined effect of noise and parameter changes on the related problem of 'attractor selection' in a noisy system.

More recently, bifurcation-driven tipping points or *dynamic bifurcations* [10] have been suggested as an important mechanism by which sudden changes in the behaviour of a system may come about. For example, Lenton *et al.* [11,12] conceptualized this as an open system

$$\frac{\mathrm{d}x}{\mathrm{d}t} = f(x, \lambda(t)), \tag{1.1}$$

where $\lambda(t)$ is in general a time-varying input. In the case that λ is constant, we refer to (1.1) as the *parametrized system* with parameter λ, and to its stable solution as the *quasi-static attractor*. If $\lambda(t)$ passes through a bifurcation point of the parametrized system where a quasi-static attractor (such as an equilibrium point $\tilde{x}(\lambda)$) loses stability, it is intuitively clear that a system may 'tip' directly as a result of varying that parameter, though in certain circumstances the effect may be delayed because of well-documented slow passage through bifurcation effects [13]. Related to this, Dakos *et al.* [14] have proposed that tipping points are recognizable and to some extent predictable. They propose a method to de-trend signals and then, examining the correlation of fluctuations in the de-trended signal, they find a signature of bifurcation-induced tipping points. These papers have concentrated on systems where equilibrium solutions for the parametrized system lose stability, although recent work of Kuehn [15] considered tipping effects in general two time-scale systems as occasions when there is a bifurcation of the fast dynamics.

The explanation of climate tipping as a phenomenon purely induced by bifurcations has been called into question. For example, Ditlevsen & Johnsen [16] suggested that the predictive techniques to forecast a forthcoming tipping point [14] are not always reliable. Indeed, noise alone can drive a system to tipping without any bifurcation. Nonetheless, it seems that the ideas of bifurcation-induced tipping can give practically useful predictions; for example, in detecting potential ecosystem population collapses [17].

In their review paper, Thompson & Sieber [18] discussed bifurcation- and noise-induced mechanisms for tipping. They examined stochastically forced systems

$$\mathrm{d}x = f(x, \lambda(t))\mathrm{d}t + g(x)\mathrm{d}W, \tag{1.2}$$

where W represents a Brownian motion. Using generic bifurcation theory, they distinguished between *safe bifurcations* (where an attracting state loses stability but is replaced by another 'nearby' attractor), *explosive bifurcations* (where the attractor dynamics explores more of phase space but still returns to near the old attractor) and *dangerous bifurcations* (where the attractor dynamics after bifurcation are unrelated to what has gone before). Thompson & Sieber [19] clarified that a time-series analysis of a bifurcation-induced tipping point near a quasi-static equilibrium (QSE) relies on a separation of time scales

$$\kappa_{\mathrm{drift}} \ll \kappa_{\mathrm{crit}} \ll \kappa_{\mathrm{stab}}, \tag{1.3}$$

where κ_{drift} is the average drift rate of parameters, κ_{crit} is the decay rate for the slowest decaying mode of the QSE and κ_{stab} are the remaining (faster decaying) modes. However, it is not easy to define κ_{drift} in general (especially in a coordinate-independent manner) and there is no *a priori* reason for inequality (1.3) to hold for a given system.

Rate-dependent tipping has not previously been discussed in detail, but it has been identified in Wieczorek *et al.* [20] as an important tipping mechanism that cannot be explained by previously proposed mechanisms (i.e. noise or bifurcations of a quasi-static attractor). This paper aims to better understand the phenomenon of rate-dependent tipping by introducing a linear model with a *tipping radius* and discussing three basic examples where this type of tipping appears.

We suggest that tipping effects in open systems can be usefully split into three categories:

— 'B-tipping', in which the output from an open system changes abruptly or qualitatively owing to a bifurcation of a quasi-static attractor.
— 'N-tipping', in which noisy fluctuations result in the system departing from a neighbourhood of a quasi-static attractor.
— 'R-tipping', in which the system fails to track a continuously changing quasi-static attractor.

We demonstrate that each mechanism *on its own* can produce a tipping response. Furthermore, any open system may exhibit tipping phenomena that result from a combination of several of the above.

This paper is organized as follows: in the remainder of this section, we discuss a setting for open systems, allowing discussion of the three types of tipping phenomena. In §2, we formulate a criterion for R-tipping. In §3, we discuss three illustrative low-dimensional examples of R-tipping; two related to bifurcation normal forms and one for a slow–fast system. Section 4 gives an illustrative example of all three types of tipping for an energy-balance model of the global climate for different parameter regimes. Section 5 concludes with a discussion and some open questions.

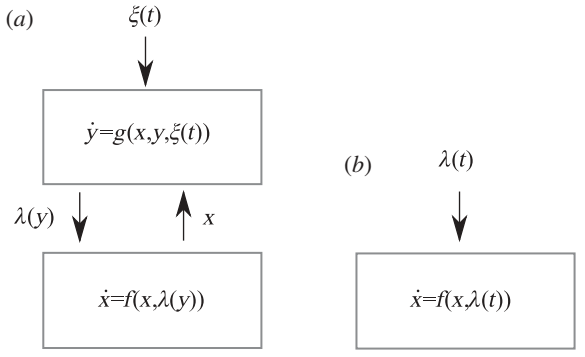

Figure 1. The system (x, y) in (a) represents a (high dimensional) open system with inputs $\xi(t)$. We identify a low-dimensional but nonlinear subsystem x forced by some 'observables' $\lambda(y)$ from the high-dimensional system. The behaviour of x in (a) can be partially understood by examining the open subsystem (b) for a suitable class of temporal forcing $\lambda(t)$.

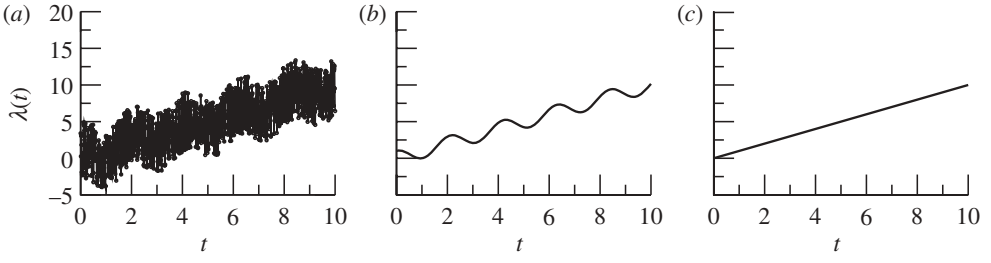

Figure 2. Candidate inputs $\lambda(t)$ in the subsystem (1.1). These may include noise- and signal-like components as in (a), or purely deterministic smooth inputs/parameter variations as in (b,c). Tipping responses in the subsystem may occur in response to noise fluctuations (N-tipping), to passing through a bifurcation point for the parametrized subsystem $\lambda = \lambda_0$ (B-tipping) or as a result of too rapid variation (R-tipping).

(*a*) *Towards a general theory of tipping in open systems*

Dynamical systems theory has developed a wide-ranging corpus of results concentrated on the behaviour of autonomous finite-dimensional deterministic systems—often called *closed systems*, because their future time trajectories depend only on the current state of the system. If the systems have inputs that can change the fate of system trajectories then we say the system is *open*. Real-world systems are never closed except to some degree of approximation, and a range of methods have been developed to cope with the fact that they are open: (i) one can view external perturbations as time variation of parameters that would be fixed for a closed system; (ii) there are various theoretical approaches to stochasticity in systems, either intrinsic or external; and (iii) control theory allows one to design inputs to control a system's outputs in a desired way, given (possibly imperfect) knowledge of the system.

In figure 1*a*, we illustrate an arbitrary high-dimensional system where we have identified a low-dimensional subsystem that we wish to check for 'tipping effects'. We do this by analysing the response of an open system (1.1) in figure 1*b* to possible time-varying inputs $\lambda(t)$. Figure 2 shows some possible candidates for

the input $\lambda(t)$; we are interested in classifying those inputs that lead to a sudden change in x. This 'tipping' may depend on details of the noise (N-tipping), may involve passing through a critical value of $\lambda(t)$ corresponding to a bifurcation (B-tipping) of the parametrized subsystem or may depend on the rate of change of $\lambda(t)$ along some path in parameter space (R-tipping).

2. R-tipping: a linear model

We use a simple model to explore R-tipping and to give sufficient conditions such that R-tipping does/does not occur. Suppose that the system (1.1) for $x \in \mathbb{R}^n$ and parameter λ has a *QSE* $\tilde{x}(\lambda)$ with a *tipping radius* $R > 0$. For some initial x_0 with $|x_0 - \tilde{x}(\lambda)| < R$, we assume that the evolution of x with time is given by

$$\frac{\mathrm{d}x}{\mathrm{d}t} = M(x - \tilde{x}(\lambda)) \quad \text{for} \quad |x - \tilde{x}(\lambda)| < R, \tag{2.1}$$

where M is a fixed stable linear operator (i.e. $|\mathrm{e}^{Mt}| \to 0$ as $t \to \infty$). More generally, we consider a time-varying parameter, $\lambda(t)$, that represents the input to the subsystem. If $|x(t) - \tilde{x}(\lambda(t))| < R$ then we say that $x(t)$ *tracks* (or adiabatically follows) the QSE $\tilde{x}(\lambda)$. If there is a t_0 such that $|x(t_0) - \tilde{x}(\lambda(t_0))| = R$ then we say the solution *tips* (adiabatic approximation fails) at t_0 and regard the model as unphysical beyond this point in time. The tipping radius may be related to the basin of attraction boundary for the nonlinear problem (1.1), as is the case in §3*a*,*b*, but it need not be, as is the case in §3*c* and in Wieczorek *et al.* [20]. System (2.1) shows only R-tipping—because M is fixed there is no bifurcation in the system and no noise is present. Clearly, the model can be generalized to include M and R that vary with $\lambda(t)$, and/or nonlinear terms. Equation (2.1) can be solved with initial condition $x(0) = x_0$ to give

$$x(t) = \mathrm{e}^{Mt}x_0 + \int_{s=0}^{t} \mathrm{e}^{M(t-s)} M\tilde{x}(\lambda(s))\mathrm{d}s.$$

If we assume that the solution is modelled by the linear system near the QSE for an arbitrarily long past and set $u = t - s$, then the dependence on initial value decays to give

$$x(t) = -\int_{u=0}^{\infty} \mathrm{e}^{Mu} M\tilde{x}(\lambda(t-u))\mathrm{d}u. \tag{2.2}$$

Assuming that M is invertible and exponentially stable (more precisely, we assume that $|\mathrm{e}^{Mt}M^{-k}v| \to 0$ as $t \to 0$ for $k = 1, 2$) and that the rate of motion of the QSE and parameter are bounded (more precisely, the derivatives $\mathrm{d}^l\tilde{x}/\mathrm{d}\lambda^l$ and $\mathrm{d}^l\lambda/\mathrm{d}t^l$ for $l = 1, 2$ are bounded in time) then (2.2) can be integrated by parts to give

$$x(t) = -\left[\mathrm{e}^{Mu}\tilde{x}(\lambda(t-u))\right]_0^{\infty} - \int_0^{\infty} \mathrm{e}^{Mu}\frac{\mathrm{d}\tilde{x}}{\mathrm{d}t}(\lambda(t-u))\mathrm{d}u$$

and so

$$x(t) - \tilde{x}(\lambda(t)) = -\int_0^{\infty} \mathrm{e}^{Mu}\frac{\mathrm{d}\tilde{x}}{\mathrm{d}t}(\lambda(t-u))\mathrm{d}u. \tag{2.3}$$

Integrating again by parts gives

$$\begin{aligned} x(t) - \tilde{x}(t) &= M^{-1}\frac{\mathrm{d}\tilde{x}}{\mathrm{d}t}(\lambda(t)) - \int_0^\infty \mathrm{e}^{Mu} M^{-1}\frac{\mathrm{d}^2\tilde{x}}{\mathrm{d}t^2}(\lambda(t-u))\mathrm{d}u \\ &= L(t) + E(t). \end{aligned}$$

The linear instantaneous lag is

$$L(t) = M^{-1}\frac{\mathrm{d}\tilde{x}}{\mathrm{d}t}(\lambda(t)). \tag{2.4}$$

If we define the *drift* of the QSE to be the rate of change

$$r(t) := \frac{\mathrm{d}\tilde{x}}{\mathrm{d}t} = \frac{\mathrm{d}\tilde{x}}{\mathrm{d}\lambda}\frac{\mathrm{d}\lambda}{\mathrm{d}t} \tag{2.5}$$

then the linear instantaneous lag is

$$L(t) = M^{-1}r(t). \tag{2.6}$$

The error to the linear instantaneous lag is

$$E(t) = -\int_0^\infty \mathrm{e}^{Mu} M^{-1}\frac{\mathrm{d}^2\tilde{x}}{\mathrm{d}t^2}(\lambda(t-u))\mathrm{d}u,$$

which includes historical information. This can also be expressed as

$$E(t) = -\int_0^\infty \mathrm{e}^{Mu} M^{-1}[\tilde{x}''(\lambda(t-u))(\lambda'(t-u))^2 + \tilde{x}'(\lambda(t-u))\lambda''(t-u)]\mathrm{d}u.$$

To summarize, the solution of (2.1) follows the QSE $\tilde{x}(\lambda(t))$ with a linear instantaneous lag term $L(t)$ and a history-dependent term $E(t)$.

(*a*) *A criterion for R-tipping with steady drift*

If $\mathrm{d}\tilde{x}/\mathrm{d}t = r$ is constant in time then we say the system has *steady drift* and (2.3) simplifies to $x(t) - \tilde{x}(\lambda(t)) = M^{-1}r$. In other words, one can verify that $E(t) = 0$ and that

$$|x(t) - \tilde{x}(\lambda(t))| = |M^{-1}r|. \tag{2.7}$$

On writing the matrix norm $\|M\| = \sup_{v\neq 0} |Mv|/|v|$, we note that for any $r \neq 0$ and invertible M we have

$$\|M\|^{-1} \cdot |r| \leq |M^{-1}r| \leq \|M^{-1}\| \cdot |r|.$$

We can avoid R-tipping if $|x(t) - \tilde{x}(\lambda(t))| = |M^{-1}r| < R$, and hence a sufficient condition on the rate of parameter variation to avoid R-tipping is that

$$\|M^{-1}\| \cdot |r| < R \tag{2.8}$$

while a sufficient condition for R-tipping to occur in this model is that

$$\|M\|^{-1} \cdot |r| > R.$$

In the intermediate case, the path of parameter variation will determine whether or not there is any R-tipping.

(b) General criteria for R-tipping

In the more general case where $r(t)$ varies, we can use (2.3) to note that

$$|x(t) - \tilde{x}(t)| \leq \int_{u=0}^{\infty} \mathrm{e}^{Mu} \sup_{u \leq t} \left| \frac{\mathrm{d}\tilde{x}}{\mathrm{d}t}(\lambda(u)) \right| \mathrm{d}u.$$

If we define

$$|r_{\max}(t)| = \sup_{u \leq t} \left| \frac{\mathrm{d}\tilde{x}}{\mathrm{d}t}(\lambda(u)) \right| = \sup_{u \leq t} \left| \frac{\mathrm{d}\tilde{x}}{\mathrm{d}\lambda}(\lambda(u)) \frac{\mathrm{d}\lambda}{\mathrm{d}t}(u) \right|,$$

then, noting that $\int_{u=0}^{\infty} \mathrm{e}^{Mu} v \, \mathrm{d}u = |M^{-1} v|$, we can guarantee that (2.1) avoids R-tipping up to time t if

$$\|M^{-1}\| \cdot |r_{\max}(t)| < R. \tag{2.9}$$

Conversely, there will be an R-tipping by time t if

$$\|M\|^{-1} = \frac{R}{|r_{\max}(t)|} = R \left(\sup_{u \leq t} \left| \frac{\mathrm{d}\tilde{x}}{\mathrm{d}\lambda} \frac{\mathrm{d}\lambda}{\mathrm{d}t} \right| \right)^{-1}. \tag{2.10}$$

One can define a natural time scale for the motion of the QSE as

$$\frac{R}{|r(t)|} = R \left(\left| \frac{\mathrm{d}\tilde{x}}{\mathrm{d}\lambda} \frac{\mathrm{d}\lambda}{\mathrm{d}t} \right| \right)^{-1};$$

note that, in general, combinations of $\mathrm{d}\tilde{x}/\mathrm{d}t$ and $\mathrm{d}\lambda/\mathrm{d}t$ do not give time scales in units per second. For an R-tipping to occur, this natural time scale may be comparable to the slowest time scale (e.g. the reciprocal of the leading eigenvalue of M) of the parametrized system. The three examples in §3 have $|\mathrm{d}\tilde{x}/\mathrm{d}\lambda| = 1$ and $R \approx 1$ so we expect R-tipping when $|\mathrm{d}\lambda/\mathrm{d}t| \approx \|M\|$. However, if $|\mathrm{d}\tilde{x}/\mathrm{d}\lambda| \approx 1/\epsilon$, then clearly we can have R-tipping even when $|\mathrm{d}\lambda/\mathrm{d}t| \approx \epsilon\|M\|$.

It is possible to think of more general tipping problems by analogy with the 'linear system and tipping radius' model discussed here. For example, for an open nonlinear system, we consider an 'effective tipping radius' that corresponds to how far the linearized system needs to be from a branch of QSE to ensure that the nonlinear system tips. There is however no exact analogy possible—the effective tipping radius may depend on the shape of the local basin of attraction, the nonlinearities present and the exact path taken in parameter space.

3. R-tipping: model examples

We give three illustrative examples of R-tipping. The first two are based on normal forms for the two basic co-dimension one bifurcations that are generic for dissipative systems: the saddle–node and the Hopf bifurcation. The third is an example that uses a fast–slow system to show that R-tipping can occur even in cases where there is a single attractor that is globally asymptotically stable.

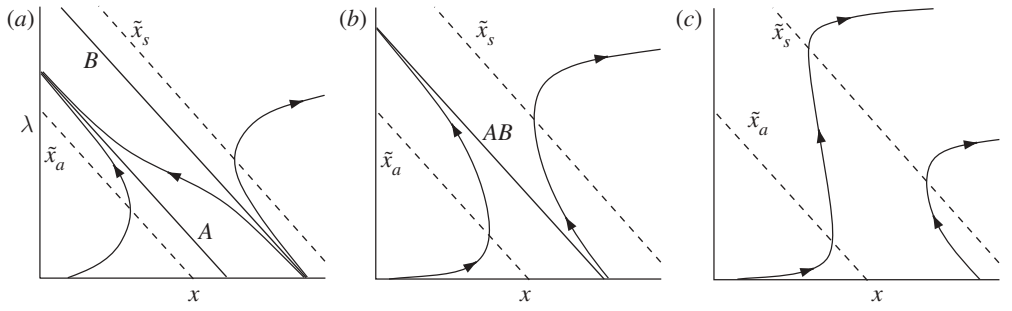

Figure 3. Phase portraits of (3.1) for (*a*) $0 < r < \mu$, (*b*) $r = \mu$, and (*c*) $r > \mu$, including the two quasi-static equilibria, $\tilde{x}_a$ and $\tilde{x}_s$, and the two invariant lines, A and B.

(*a*) *Saddle–node normal form with steady drift*

We consider the example system for $x \in \mathbb{R}$ with parameter $\lambda(t) \in \mathbb{R}$ and drift r,

$$\frac{\mathrm{d}x}{\mathrm{d}t} = (x + \lambda)^2 - \mu \tag{3.1}$$

and

$$\frac{\mathrm{d}\lambda}{\mathrm{d}t} = r, \tag{3.2}$$

with fixed $\mu > 0$. In the (x, λ) phase plane of (3.1)–(3.2), there are two $\mathrm{d}x/\mathrm{d}t = 0$ isoclines given by $\tilde{x}_a(\mu) = \{(x, \lambda) \in \mathbb{R}^2 : \lambda = -\sqrt{\mu} - x\}$ and $\tilde{x}_s(\mu) = \{(x, \lambda) \in \mathbb{R}^2 : \lambda = \sqrt{\mu} - x\}$ that correspond to two QSE: a stable node and a saddle, respectively, for (3.1). Furthermore, if $\mu > r$ there are two invariant lines, one attracting

$$A(\mu, r) = \{(x, \lambda) \in \mathbb{R}^2 : \lambda = -\sqrt{\mu - r} - x\}$$

and one repelling

$$B(\mu, r) = \{(x, \lambda) \in \mathbb{R}^2 : \lambda = \sqrt{\mu - r} - x\},$$

both with a constant slope $\mathrm{d}\lambda/\mathrm{d}x = -1$ (figure 3). The stability manifests itself as an exponential decay (growth) of small perturbations about $A(\mu, r)$ ($B(\mu, r)$).

If $0 < r < \mu$ then $B(\mu, r)$ defines a *tipping threshold*. Initial conditions below $B(\mu, r)$ converge to $A(\mu, r)$, whereas initial conditions above $B(\mu, r)$ give rise to solutions $x(t) \to \infty$ as $t \to \infty$. If $r = \mu$ then $A(\mu, r)$ and $B(\mu, r)$ coalesce into a neutrally stable invariant line AB (figure 3*b*) that disappears for $r > \mu$ (figure 3*c*). Hence, for $r > \mu$ there is no tipping threshold, meaning that trajectories for all initial conditions become unbounded as $t \to \infty$.

Let us assume that the system is at (x_0, λ_0) at time $t = 0$. If the initial condition (x_0, λ_0) lies between $\lambda = -x$ and $\tilde{x}_s(\mu)$, then the critical rate r_c is the value of r at which the r-dependent tipping threshold $B(\mu, r)$ crosses (x_0, λ_0). If the initial condition lies on or below the line $\lambda = -x$ then the critical rate r_c is the value of r at which $B(\mu, r)$ and $A(\mu, r)$ meet and disappear. This gives a precise value for the critical rate as the following function of initial conditions:

$$r_\mathrm{c} = \begin{cases} \mu - (\lambda_0 + x_0)^2 & \text{if } -x_0 < \lambda_0 < -x_0 + \sqrt{\mu}, \\ \mu & \text{if } \lambda_0 \leq -x_0. \end{cases} \tag{3.3}$$

We can approximate this result using the simple linear model (2.1) with the linearization at the QSE as $M=-2\sqrt{\mu}$ so that $\|M^{-1}\|=\|M\|^{-1}=1/(2\sqrt{\mu})$. Clearly, the linear model with $R=2\sqrt{\mu}$ given by $\tilde{x}_s$ (basin boundary for $\tilde{x}_a$) overestimates r_c because the linear attraction weakens on moving away from the stable QSE in the nonlinear problem. This can be overcome by choosing an *effective tipping radius* R_c. Comparing with (2.8), the system avoids tipping if

$$|r|<2\sqrt{\mu}R_c,$$

which, for $r_c=\mu$, suggests an effective tipping radius $R_c=\sqrt{\mu}/2$. Finally, owing to steady drift, this problem can be reduced to a saddle–node bifurcation at $r=\mu$ in a co-moving coordinate system $y=x+\lambda$.

(*b*) *A subcritical Hopf normal form*

As a second example, we consider

$$\frac{\mathrm{d}z}{\mathrm{d}t}=F(z-\lambda), \tag{3.4}$$

where $z=x+\mathrm{i}y\in\mathbb{C}$. For the subcritical Hopf normal form with frequency ω, we choose

$$F(z)=(-1+\mathrm{i}\omega)z+|z|^2z.$$

Note that the system (3.4) has only one QSE at $\tilde{z}=\lambda(t)$. Two cases of R-tipping that we consider are with steady drift (these can be reduced to a bifurcation problem in another coordinate system) and with unsteady drift (where there is no straightforward simplification to a bifurcation problem).

(i) *Hopf normal form with steady drift*

Consider (3.4) with a uniform drift of the QSE along the real axis, at a rate r (which must be real): $\mathrm{d}\lambda/\mathrm{d}t=r$. There is a critical rate r_c at which the system moves away from the stable QSE. We can find this r_c analytically by changing to the co-moving system for $w=z-\lambda$,

$$\frac{\mathrm{d}w}{\mathrm{d}t}=F(w)-r, \tag{3.5}$$

where a stable equilibrium represents the ability to track the QSE in the original system. Setting $w=|w|\,\mathrm{e}^{\mathrm{i}\theta}$ and rewriting equation (3.5) in terms of $\mathrm{d}|w|/\mathrm{d}t$ and $\mathrm{d}\theta/\mathrm{d}t$ gives an equilibrium at $(|w_e|,\theta_e)$ that satisfies

$$|w_e|^6-2|w_e|^4+(\omega^2+1)|w_e|^2-r^2=0. \tag{3.6}$$

In the (r,ω) parameter plane, there is a saddle–node bifurcation curve (S in figure 4*a*) whose different branches are given by equation (3.6) with

$$|w_e|^2_{\pm}=\frac{2}{3}\left(1\pm\sqrt{1-\frac{3}{4}(1+\omega^2)}\right), \tag{3.7}$$

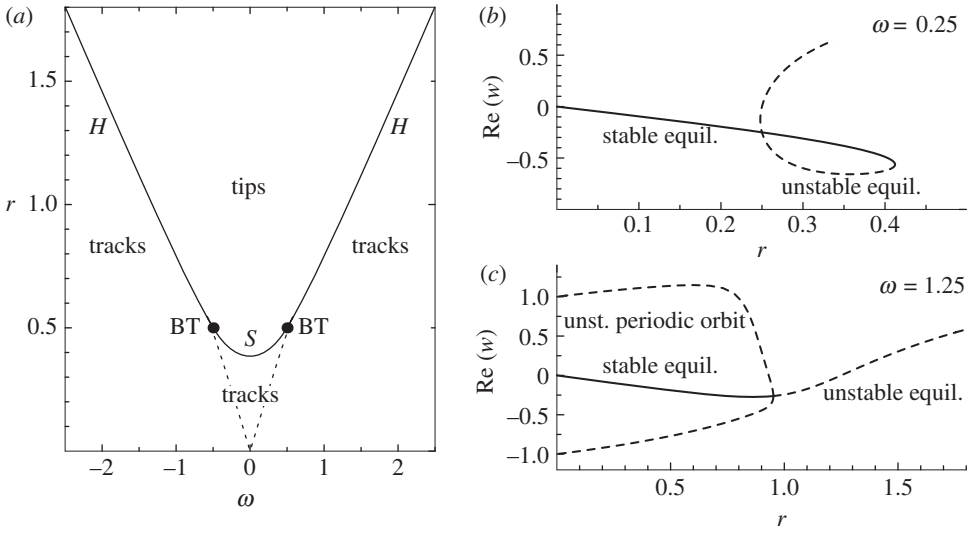

Figure 4. (*a*) Solid curves in a two-parameter tipping diagram for (3.4) with steady drift indicate the critical rate $r_c(\omega)$. The stable equilibrium for the co-moving system (3.5), or the ability to track the QSE in the original system (3.4), (*b*) disappears in a saddle–node bifurcation or (*c*) destabilizes in a subcritical Hopf bifurcation when $r = r_c(\omega)$.

and join at cusp points at $(r, \omega) = (\pm(2/3)^{3/2}, \pm(1/3)^{1/2})$ (not marked in figure 4*a*). Linearizing about the stable equilibrium $(|w_e|, \theta_e)$ reveals that the characteristic polynomial

$$s^2 + (2 - 4|w_e|^2)s + \omega^2 + (|w_e|^2 - 1)(3|w_e|^2 - 1) = 0$$

has a pair of pure imaginary roots, indicating a Hopf bifurcation when $|w_e|^2 = 1/2$ and $\omega^2 > 1/4$. In the (r, ω) parameter plane, (disjoint) Hopf bifurcation curves (H) originate from Bogdanov–Takens bifurcation points (BT) at $(r, \omega) = (\pm 1/2, \pm 1/2)$, and are given by

$$\frac{1 + 4\omega^2}{8} - r^2 = 0 \quad \text{and} \quad \omega^2 > \frac{1}{4}, \tag{3.8}$$

which follows from equation (3.6) with $|w_e|^2 = 1/2$. At BT, saddle–node bifurcation changes from super (solid) to subcritical (dashed). It turns out that the stable equilibrium for (3.5), indicating the ability to track the QSE in the original system, disappears in a supercritical saddle–node bifurcation when $\omega^2 < 1/4$ and becomes unstable in a subcritical Hopf bifurcation when $\omega^2 > 1/4$. Hence, for initial conditions within the basin boundary of this equilibrium, the critical rate is given by

$$r_c(\omega) = \begin{cases} \pm\sqrt{|w_e|_-^6 - 2|w_e|_-^4 + (\omega^2 + 1)|w_e|_-^2} & \text{if } \omega^2 \le \dfrac{1}{4}, \\ \pm\sqrt{\dfrac{(1 + 4\omega^2)}{8}} & \text{if } \omega^2 > \dfrac{1}{4}. \end{cases} \tag{3.9}$$

Again, we can approximate this result using the simple linear model (2.1) with the linearization at the QSE as $M = (-1, 5; -5, -1)$ so that $\|M^{-1}\| = \|M\|^{-1} = 0.1961$. Clearly, the linear model with a tipping radius $R = 1$ given by the unstable periodic orbit (basin boundary for $\tilde{z}$) does not account for nonlinear attraction away from the QSE and for the spiralling shape of trajectories when $\omega \neq 0$. Therefore, we choose an effective tipping radius R_c. Comparing with (2.8), the system avoids tipping if

$$|r| < 5.0990 R_c,$$

which suggests an ω-dependent effective tipping radius $R_c(\omega) = r_c(\omega)/5.099$.

R-tipping that reduces to a bifurcation problem in a co-moving system should not be confused with B-tipping: observe that the bifurcation parameter r does not vary in time, and it is 'the ability to track the QSE', rather than the QSE itself, that bifurcates.

(ii) *Hopf normal form with unsteady drift*

We now consider (3.4) where we include a smooth shift of QSE between asymptotically steady positions at $z = 0$ to $z = \Delta$, according to

$$\frac{\mathrm{d}\lambda}{\mathrm{d}t} = \rho\lambda(\Delta - \lambda), \quad \lambda(t_0) = \frac{\Delta}{2}, \tag{3.10}$$

where $\rho > 0$ parametrizes the *maximum rate of the shift*, $\Delta > 0$ is the amplitude of the shift and t_0 is the time when the rate of change is largest. Integrating (3.10) gives

$$\lambda(t) = \Delta \frac{(\tanh(\Delta\rho(t - t_0)/2) + 1)}{2}, \tag{3.11}$$

which implies the following parameter dependence on time:

$$\lambda(-t) \to 0, \ \lambda(t) \to \Delta \quad \text{as} \ \ t \to \infty \quad \text{and} \quad \frac{\mathrm{d}\lambda}{\mathrm{d}t} \leq \frac{\mathrm{d}\lambda}{\mathrm{d}t}(t_0) = \frac{\Delta^2\rho}{4}.$$

Near $t = t_0$ this describes a smooth shift between the location of an asymptotically stable equilibrium from $z = 0$ to $z = \Delta$, and the maximum rate of the shift is $\Delta^2\rho/4$ at $t = t_0$. Observe that there is no change in stability or basin size of the QSE as t changes. Figure 5 shows typical trajectories starting at an arbitrary initial condition within the basin of attraction using fixed Δ and two values of ρ. As shown in the diagram, there is a critical value ρ_c such that for $\rho < \rho_c$ the system can track the QSE while for $\rho > \rho_c$ a tipping occurs near $t = t_0$.

J. Sieber (2010, personal observation) has pointed out that this case may still be quantifiable by numerical approximation of the ρ_c that gives a heteroclinic connection from an (initial) saddle equilibrium at $(z, \lambda) = (0, 0)$ to a saddle periodic orbit at $(|z - \Delta|, \lambda) = (1, \Delta)$ for the extended system (3.4) and (3.10). Such a connection indicates ρ_c for which the (initial) saddle equilibrium moves away from the basin boundary of the stable equilibrium at $(z, \lambda) = (\Delta, \Delta)$.

(c) *A fast–slow system with R-tipping*

A particularly interesting case of R-tipping can occur in slow–fast systems that have a (unique, globally stable) QSE near a locally folded critical (slow) manifold,

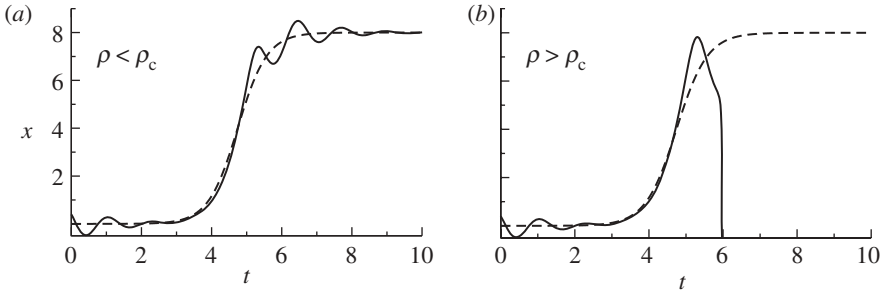

Figure 5. R-tipping for (3.5)–(3.10) for $\Delta = 8$ showing time evolution for (*a*) $\rho = 4.76$ and (*b*) $\rho = 4.8$ (recall that ρ scales the maximum rate of change) from an initial condition $(x, y, \lambda) = (0.4, 0.5, 0.0001)$. For $\rho > \rho_c = 4.78$, we find that system trajectories no longer follow the stable QSE (shown by the dashed line) as they meet its basin boundary.

of which the recently studied compost-bomb instability is a representative [20,21]. Here, we consider a simple example

$$\epsilon \frac{\mathrm{d}x_1}{\mathrm{d}t} = x_2 + \lambda + x_1(x_1 - 1) \tag{3.12}$$

and

$$\frac{\mathrm{d}x_2}{\mathrm{d}t} = -\sum_{n=1}^{N} x_1^n, \tag{3.13}$$

with odd N, fast variable $x_1 \in \mathbb{R}$, slow variable $x_2 \in \mathbb{R}$, and small parameter $0 < \epsilon \ll 1$. A unique equilibrium for (3.12)–(3.13), $\tilde{x}(\lambda) = (0, -\lambda)$, is asymptotically stable for any fixed value of λ, and globally asymptotically stable if $N \geq 5$. The slow dynamics is approximated by the one-dimensional *critical* (*slow*) *manifold*, $S(\lambda) = \{(x_1, x_2) \in \mathbb{R}^2 : x_2 = -\lambda - x_1(x_1 - 1)\}$, that has a fold, $L(\lambda) = (\frac{1}{2}, -\lambda + \frac{1}{4})$, tangent to the fast x_1 direction. If $N \geq 5$, the fold defines a tipping threshold that is not associated with any basin boundary. Here, $S(\lambda)$ is partitioned into the attracting part, $S_a(\lambda)$ for $x_1 < \frac{1}{2}$, fold $L(\lambda)$ for $x_1 = \frac{1}{2}$, and repelling part, $S_r(\lambda)$ for $x_1 > \frac{1}{2}$.

(i) *The slow–fast system with steady drift*

Consider (3.12)–(3.13) with a uniform drift of the QSE, $\tilde{x}(\lambda(t))$, in the negative x_2 direction at a constant rate

$$\frac{\mathrm{d}\lambda}{\mathrm{d}t} = r > 0, \tag{3.14}$$

so that λ becomes the second slow variable. There is a critical rate, r_c, at which (3.12)–(3.14) is destabilized, meaning that trajectories diverge away from the QSE for $r > r_c$. We can find this critical rate in the singular limit, $\epsilon \to 0$,

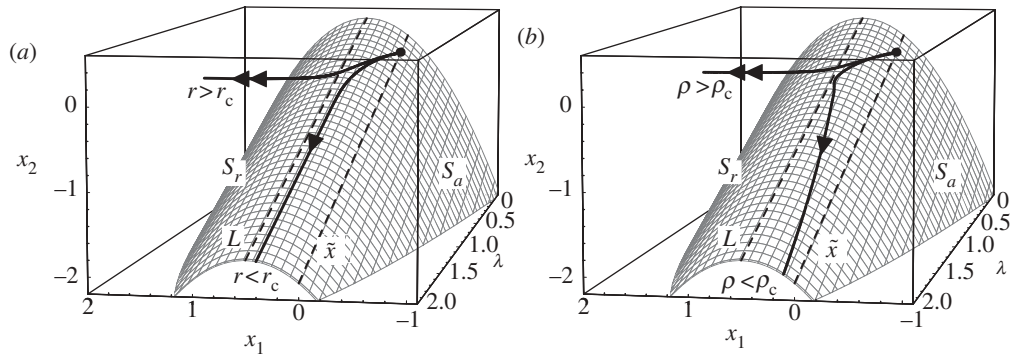

Figure 6. R-tipping in slow–fast systems with a unique QSE, $\tilde{x}$, and (grey surface) locally folded critical (slow) manifold, $S = S_a \cup L \cup S_r$, for (*a*) the steady drift problem (3.12)–(3.14) and (*b*) the unsteady drift problem (3.12)–(3.13) and (3.20), where $\epsilon = 0.01$ and $N = 1$. In (*a*), equation (3.19) gives $r_c = \frac{1}{2}$ and shown are trajectories for $r = 0.4 < r_c$ and $r = 0.6 > r_c$. In (*b*), equation (3.23) gives $\rho_c \approx 0.99$ for the initial condition at the origin (black dot) and shown are trajectories for $\rho = 0.7 < \rho_c$ and $\rho = 1 > \rho_c$.

by setting $\epsilon = 0$ in (3.12), differentiating the resulting algebraic equation with respect to t, and studying the *projected reduced system* [22],

$$\frac{\mathrm{d}x_1}{\mathrm{d}t} = \left(-r + \sum_{n=1}^{N} x_1^n\right)(2x_1 - 1)^{-1} \tag{3.15}$$

and

$$\frac{\mathrm{d}\lambda}{\mathrm{d}t} = r, \tag{3.16}$$

that approximates the slow dynamics for (3.12)–(3.14) on the two-dimensional critical manifold, $S = \{(x_1, x_2, \lambda) \in \mathbb{R}^3 : x_2 = -\lambda - x_1(x_1 - 1)\}$ (grey surface in figure 6). Although (3.15)–(3.16) is typically singular at the one-dimensional fold, $L = \{(x_1, x_2, \lambda) \in \mathbb{R}^3 : x_1 = \frac{1}{2}, x_2 = -\lambda + \frac{1}{4}\}$, its phase portrait can be constructed by rescaling time

$$\frac{\mathrm{d}t}{\mathrm{d}\tau} = -(2x_1 - 1) \Rightarrow t = -\int_0^\tau (2x_1(s) - 1)\mathrm{d}s,$$

producing the phase portrait for the *desingularized system* [23]

$$\frac{\mathrm{d}x_1}{\mathrm{d}\tau} = r - \sum_{n=1}^{N} x_1^n \tag{3.17}$$

and

$$\frac{\mathrm{d}\lambda}{\mathrm{d}\tau} = -r(2x_1 - 1), \tag{3.18}$$

and then reversing the direction of time on the repelling part of the critical manifold, S_r. In this way, we find that for $0 < r < \sum_{n=1}^{N} 2^{-n}$ trajectories for all initial conditions within S_a converge to a stable invariant line that is defined by a constant x_1 satisfying $r = \sum_{n=1}^{N} x_1^n$, meaning that trajectories remain close to the

QSE, $\tilde{x}$, for all time $[r < r_c]$ in figure 6*a*. However, for $r > \sum_{n=1}^{N} 2^{-n}$, trajectories for all initial conditions within S_a reach the fold, L, where they 'slip off' the critical manifold and diverge away from the QSE in the fast x_1 direction $[r > r_c]$ in figure 6*a*. Hence, system (3.12)–(3.14) exhibits R-tipping and, for $\epsilon \to 0$, the critical rate is

$$r_c = \sum_{n=1}^{N} 2^{-n}. \tag{3.19}$$

(ii) *The slow–fast system with unsteady drift*

We now consider (3.12)–(3.13) with a non-uniform drift

$$\frac{d\lambda}{dt} = \rho\, e^{-\lambda} \tag{3.20}$$

that is a logarithmic growth, $\lambda(t) = \ln[\rho(t - t_0) + e^{\lambda(t_0)}]$, where we assume $\rho > 0$. Again, there is a critical rate, ρ_c, at which system (3.12)–(3.13) and (3.20) is destabilized. The key difference from the steady drift problem is that ρ_c depends on the initial condition within S_a. This is because the desingularized system

$$\frac{dx_1}{d\tau} = e^{-\lambda}\rho - \sum_{n=1}^{N} x_1^n \tag{3.21}$$

and

$$\frac{d\lambda}{d\tau} = -e^{-\lambda}\rho(2x_1 - 1) \tag{3.22}$$

has a saddle equilibrium for all $\rho > 0$, corresponding to a *folded saddle singularity* [24,25],

$$F = (x_{1,F}, \lambda_F(\rho)) = \left(\frac{1}{2}, -\ln \sum_{n=1}^{N} \frac{2^{-n}}{\rho}\right),$$

for the projected reduced system. One can use the theory developed in Wieczorek *et al.* [20, §4] to approximate the critical value, ρ_c. Given F, the eigenvector

$$w = \left(-\frac{q}{p} + \sqrt{2 + \left(\frac{q}{p}\right)^2}, 1\right)^{\mathrm{T}}$$

corresponding to the stable eigendirection of the saddle F for (3.21)–(3.22), an initial condition $(x_{1,0}, \lambda_0)$ within S_a, and as far as $\epsilon \to 0$, the critical rate can be calculated using Wieczorek *et al.* [20, eqn (4.12)] to give

$$\rho_c \approx p \exp\left(\lambda_0 + \frac{1/2 - x_{1,0}}{-q/p + \sqrt{2 + (q/p)^2}}\right), \tag{3.23}$$

where $p = \sum_{n=1}^{N} 2^{-n}$, $q = \sum_{n=1}^{N} n2^{-n}$. Below the critical rate, the trajectory misses the fold, L, and approaches the QSE, $\tilde{x}$, as time tends to infinity $[\rho < \rho_c]$ in figure 6*b*. Above the critical rate, the trajectory reaches L and diverges from the

QSE in the fast x_1 direction [$\rho > \rho_c$] in figure 6*b*. Note that, in this example, the critical rate of parameter variation is of the same order as the *slow* dynamics—only when the parameter variation is *very slow* with respect to the slow variable and there are three time scales is tracking guaranteed. In this sense, the rate-dependent tipping occurs when the slow and very slow time scales are no longer separable.

4. B-, N- and R-tipping examples in a simple climate model

We present a simple climate model that independently shows, under differing circumstances, all three types of tipping. In its deterministic version, this is a 'zero-dimensional' global energy balance model originally introduced by Fraedrich [5],

$$c\frac{\mathrm{d}T}{\mathrm{d}t} = R\downarrow - R\uparrow . \tag{4.1}$$

The state variable T represents an average surface temperature of an ocean on a spherical planet subject to radiative heating. Equation (4.1) is a deterministic energy conservation law where the constant c represents the thermal capacity of a well-mixed ocean layer of depth 30 m covering 70.8 per cent of the Earth's surface. The incoming solar radiation $R\downarrow$ and outgoing radiation $R\uparrow$ are modelled as

$$R\downarrow = \tfrac{1}{4}\mu I_0(1-\alpha_p(T)) \quad \text{and} \quad R\uparrow = e_{\mathrm{SA}}\sigma T^4.$$

Here I_0 is the solar constant and the parameter μ allows for variations in the planetary orbit, or in the solar constant. An ice–albedo feedback is introduced to link variations in temperature with changes of ice and thus of albedo α_p: Fraedrich [5] used a quadratic relation

$$\alpha_p(T) = a_2 - b_2 T^2, \tag{4.2}$$

where the parameters $a_2 > 1$ and b_2 control the albedo magnitude and slope of the albedo–temperature relation. The outgoing radiation term is obtained by the Stefan–Boltzmann law, where e_{SA} is the effective emissivity and σ is the Stefan–Boltzmann constant. With these choices (4.1) is written as [5, eqn 4.1]

$$\left.\begin{aligned} \frac{\mathrm{d}T}{\mathrm{d}t} &= f(T) = c^{-1}a(-T^4 + b_\mu T^2 - d_\mu) \\ \text{and} \qquad a &= \frac{e_{\mathrm{SA}}\sigma}{c},\ b_\mu = \frac{\mu I_0 b_2}{4e_{\mathrm{SA}}\sigma},\ d_\mu = -\frac{\mu I_0(1-a_2)}{4e_{\mathrm{SA}}\sigma}. \end{aligned}\right\} \tag{4.3}$$

Table 1 shows the values of constants and parameters for the system at equilibrium. Sutera [4] reformulated Fraedrich's model to incorporate stochastic forcing:

$$\mathrm{d}T = f(T)\mathrm{d}t + \sqrt{\nu}\,\mathrm{d}W, \tag{4.4}$$

with $f(T)$ as in (4.3), where $\mathrm{d}W$ is a normalized Wiener (white noise) process such that $(\mathrm{d}W)^2$ has dimension of time t, ν has dimension of $1/t$ and the variance of $\sqrt{\nu}\,\mathrm{d}W$ per unit time is ν.

For μ larger than a critical value $0 < \mu_c < 1$, the deterministic system (4.3) has two equilibria, T^+ (stable) and T^- (unstable). A saddle–node bifurcation takes

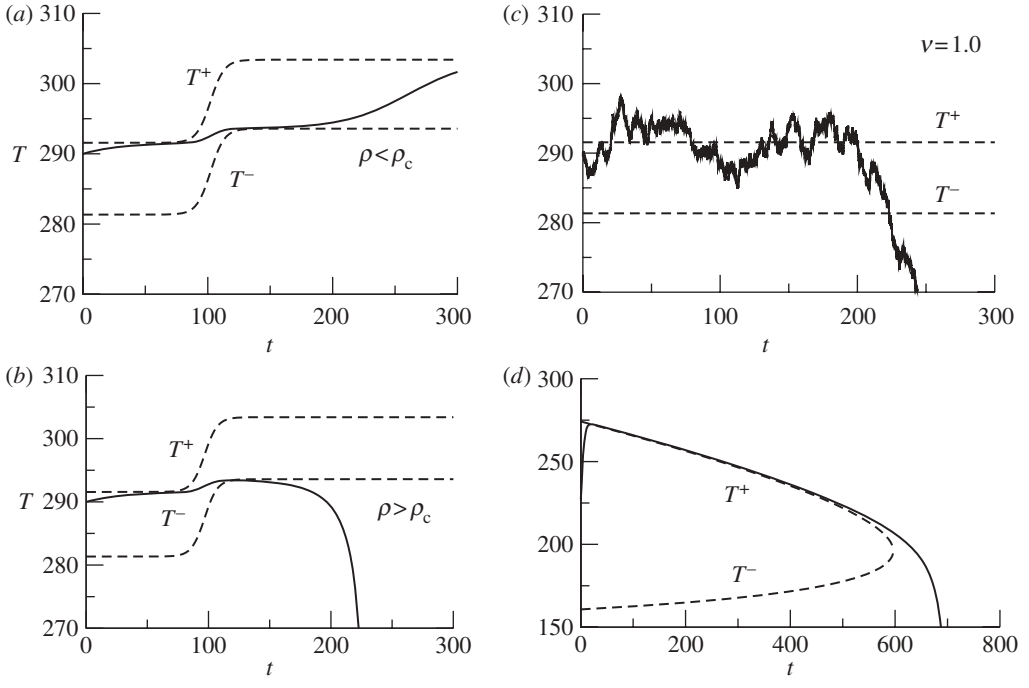

Figure 7. Illustrations of trajectories for the Sutera–Fraedrich model (4.4) showing the presence of all three tipping types for parameters in table 2—horizontal axis, years; vertical axis, Kelvin. The solid lines show system trajectories while the dashed lines show the location of the QSE—the branch T^+ is stable while the branch T^- is unstable in this model. (a,b) R-tipping for a smooth change of parameters between two steady states. (a) The system returns to the QSE after a transient ($\rho = 0.18$). (b) The system becomes unbounded, indicating a critical value $\rho_c \approx 0.185$ yr^{-1} ($\rho = 0.19$). (c) An example of N-tipping in the presence of noise of amplitude $\nu = 1.0$ yr^{-1}; (d) shows an example of B-tipping on decreasing μ uniformly from 1 at a constant rate. Note that in case (d) the two QSE coalesce at a saddle–node bifurcation.

Table 1. Values of the constants and parameters for equation (4.3).

I_0	1366 $\mathrm{W\,m^{-2}}$	μ	1
σ	5.6704×10^{-8} $\mathrm{W\,m^{-2}\,K^{-4}}$	b_2	1.690×10^{-5} $\mathrm{K^{-2}}$
c	10^8 $\mathrm{kg\,K\,s^{-2}}$	a_2	1.6927
e_{SA}	0.62		

place at some $\mu = \mu_c$ with $0 < \mu_c < 1$, where the two equilibria $T^{\pm}$ merge and disappear. Sutera [4] studied N-tipping in the stochastically forced system (4.4) for $\mu > \mu_c$, as a function of the distance $\mu - \mu_c$ from the bifurcation value. Namely, they computed the exit time such that the process jumps over the 'potential barrier' T^- and falls irreversibly to 'ice-covered Earth'.

We illustrate in figure 7 three situations where the Sutera–Fraedrich model exhibits 'pure' B-, N- and R-tipping independently; parameter values are detailed in table 2. In table 2, (a–b) shows an example of R-tipping, (c) of N-tipping and (d) of B-tipping. For case (a–b), we evolve the dimensionless parameter λ

Table 2. Parameter values for simulations shown in figure 7. For case (*a*–*b*), we interpolate between the values given along the curve such that $b_\mu^2 - 4d_\mu$ is constant at a rate proportional to ρ. In case (*c*), all parameters are fixed but noise is added, while, in case (*d*), we impose a steady drift of the parameter μ downwards.

parameter	(*a*–*b*)	(*c*)	(*d*)
μ	1.0	1.0	decreases from 1.0 at rate $-0.0004\ \mathrm{yr}^{-1}$
b_2 (K^{-2})	initial 1.690×10^{-5} final 1.8350×10^{-5}	1.690×10^{-5}	1.04×10^{-5}
a_2	initial 1.6927 final 1.8168	1.6927	1.2
ν (per year)	0	1.0	0

according to the ODE $\mathrm{d}\lambda/\mathrm{d}t = \rho\lambda(1-\lambda)$ and set $b_2 = (1-\lambda)b_2^{\mathrm{init}} + \lambda b_2^{\mathrm{final}}$—for this figure, we use initial values $\lambda = 10^6$ and $T = 290\,\mathrm{K}$. The value of a_2 is calculated to ensure that $b_\mu^2 - 4d_\mu$ is held constant for the parameter groups defined in (4.3). The constant ρ can be thought of as simply scaling the rate of passage from the initial to the final values given in the table.

5. Summary and conclusions

It is of great practical importance to understand the theoretical mechanisms behind tipping phenomena in the climate system as well as other systems. We have proposed here that such mechanisms can be effectively divided into three distinct categories: bifurcation-induced, noise-induced and rate-dependent tipping, respectively denoted as B-, N- and R-tipping. In particular, we describe R-tipping, a mechanism that may be exhibited by (subsystems of) the climate system independently of the presence or absence of the other types of tipping.

In realistic models, tipping effects may be associated with a combination of the three mechanisms, and it will be a challenge to understand this more general case. For example, B-tipping, usually associated with slow changes in a parameter, may turn into R-tipping upon increasing the rate of change for the parameters. However, as illustrated in figure 8, completely new mechanisms may appear on increasing the rate, including the possibility that B-tipping may be suppressed for fast enough variation of parameters. Alternatively, the B-tipping may persist but an R-tipping mechanism may come into play before the B-tipping is reached.

We emphasize that neither N-tipping nor R-tipping require any change of stability. Hence there is no reason to assume that the techniques of Dakos *et al.* [14], based on a de-trended autoregressive model for B-tipping, should deliver useful predictions in such cases—as noted by Ditlevsen & Johnsen [16], N-tipping is intrinsically unpredictable. We are investigating whether any novel predictive technique may be developed for R-tipping. Those cases of R-tipping that can be reduced to a local bifurcation in a co-moving system may be expected to be predictable using similar methods; this includes the examples in §3*a*,*b*(i)

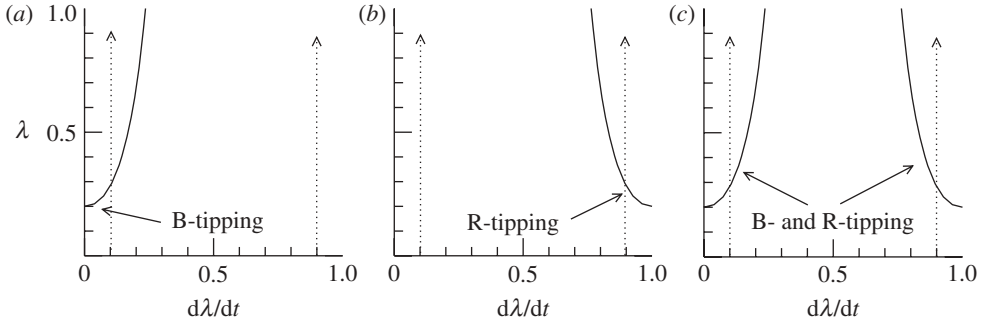

Figure 8. Different possible system behaviours on ramping the parameter λ at differing rates (dashed arrows) through the region $\lambda \in [0, 1]$. (*a*) Example where there is a B-tipping for low rates (quasi-static) that disappears for high enough rates. (*b*) An example where there is no tipping for small enough rates but R-tipping for large enough rates. (*c*) Both B- and R-tipping, but there is a range of rates where no instability appears.

with steady drift. In more complex cases, ρ_c may still be quantifiable by global heteroclinic bifurcations for an extended system, for example (3.1) and (3.10) or (3.4) and (3.10) in §3*b*(ii).

The classification proposed here may be applicable to a wide range of open systems under the influence of noise and/or parameter changes. Recent work of Nene & Zaikin [26] suggested that there may be interesting applications of rate-dependent bifurcation theory to determine cell fate. There are potentially many other application areas, from mechanics and ecology to economics and social sciences, where tipping points are of interest. We suggest that this will be an area of significant mathematical development in the coming years.

The authors thank the Isaac Newton Institute for hosting the programme 'Mathematical and Statistical Approaches to Climate Modelling and Prediction' in autumn 2010, where this topic was initially discussed, and are indebted to Alexei Zaikin and Jan Sieber for stimulating conversations in relation to this work.

References

1 Hays, J. D., Imbrie, J. & Shackleton, N. J. 1976 Variations in the Earth's orbit: pacemaker of the ice ages. *Science* **194**, 1121–1132. (doi:10.1126/science.194.4270.1121)
2 Shackleton, N. J. 2000 The 100,000-year ice-age cycle identified and found to lag temperature, carbon dioxide, and orbital eccentricity. *Science* **289**, 1897–1902. (doi:10.1126/science.289.5486.1897)
3 Hasselmann, K. 1976 Stochastic climate models. I. Theory. *Tellus* **28**, 473–485. (doi:10.1111/j.2153-3490.1976.tb00696.x)
4 Sutera, A. 1981 On stochastic perturbation and long-term climate behaviour. *Q. J. R. Meteorol. Soc.* **107**, 137–151. (doi:10.1256/smsqj.45108)
5 Fraedrich, K. 1979 Catastrophes and resilience of a zero-dimensional climate system with ice-albedo and greenhouse feedback. *Q. J. R. Meteorol. Soc.* **105**, 147–167. (doi:10.1002/qj.49710544310)
6 Mason, B. J. 1976 Towards the understanding and prediction of climatic variations. *Q. J. R. Meteorol. Soc.* **102**, 473–498. (doi:10.1002/qj.49710243302)
7 Gammaitoni, L., Hanggi, P., Jung, P. & Marchesoni, F. 1998 Stochastic resonance. *Rev. Mod. Phys.* **70**, 223–288. (doi:10.1103/RevModPhys.70.223)

8 Sura, P. 2002 Noise-induced transitions in a barotropic-plane channel. *J. Atmos. Sci.* **59**, 97–110. (doi:10.1175/1520-0469(2002)059<0097:NITIAB>2.0.CO;2)

9 Kondepudi, D. K., Moss, F. & McClintock, P. V. E. 1986 Observation of symmetry breaking, state selection and sensitivity in a noisy electronic system. *Phys. D Nonlin. Phenom.* **21**, 296–306. (doi:10.1016/0167-2789(86)90006-0)

10 Benoit, E. 1991 *Dynamic bifurcations*. Lecture Notes in Mathematics, vol. 1498. Berlin, Germany: Springer.

11 Lenton, T. M., Held, H., Kriegler, E., Hall, J. W., Lucht, W., Rahmstorf, S. & Schellenhuber, H. J. 2008 Tipping elements in the earth's climate system. *Proc. Natl Acad. Sci. USA* **105**, 1786–1793. (doi:10.1073/pnas.0705414105)

12 Lenton, T. M., Livina, V. N., Dakos, V., van Nes, E. H. & Scheffer, M. 2012 Early warning of climate tipping points from critical slowing down: comparing methods to improve robustness. *Phil. Trans. R. Soc.* **370**, 1185–1204. (doi:10.1098/rsta.2011.0304)

13 Baer, S. M., Erneux, T. & Rinzel, J. 1989 The slow passage through a hopf bifurcation: delay, memory effects and resonance. *SIAM J. Appl. Math.* **49**, 55–71. (doi:10.1137/0149003)

14 Dakos, V., Scheffer, M., van Nes, E. H., Brovkin, V., Petoukhov, V. & Held, H. 2008 Slowing down as an early warning signal for abrupt climate change. *Proc. Natl Acad. Sci. USA* **105**, 14 308–14 312. (doi:10.1073/pnas.0802430105)

15 Kuehn, C. 2011 A mathematical framework for critical transitions: bifurcations, fast–slow systems and stochastic dynamics. *Physica D* **240**, 1020–1035. (doi:10.1016/j.physd.2011.02.012)

16 Ditlevsen, P. D. & Johnsen, S. 2010 Tipping points: early warning and wishful thinking. *Geophys. Res. Lett.* **37**, L19703. (doi:10.1029/2010GL044486)

17 Drake, J. M. & Griffen, B. D. 2010 Early warning signals of extinction in deteriorating environments. *Nature* **467**, 456–459. (doi:10.1038/nature09389)

18 Thompson, J. M. T. & Sieber, J. 2011 Predicting climate tipping as a noisy bifurcation: a review. *Int. J. Bifurcation Chaos* **21**, 399–423. (doi:10.1142/S0218127411028519)

19 Thompson, J. M. T. & Sieber, J. 2010 Climate tipping as a noisy bifurcation: a predictive technique. *IMA J. Appl. Math.* **76**, 27–46. (doi:10.1093/imamat/hxq060)

20 Wieczorek, S., Ashwin, P., Luke, C. M. & Cox, P. M. 2011 Excitability in ramped systems: the compost-bomb instability. *Proc. R. Soc. A* **467**, 1243–1269. (doi:10.1098/rspa.2010.0485)

21 Luke, C. M. & Cox, P. M. 2010 Soil carbon and climate change: from the Jenkinson effect to the compost bomb instability. *Eur. J. Soil Sci.* **62**, 5–12. (doi:10.1111/j.1365-2389.2010.01312.x)

22 Fenichel, N. 1979 Geometric singular perturbation theory for ordinary differential equations. *J. Differ. Equ.* **31**, 53–98. (doi:10.1016/0022-0396(79)90152-9)

23 Krupa, M. & Szmolyan, P. 2001 Extending geometric singular perturbation theory to nonhyperbolic points—fold and canard points in two dimensions. *SIAM J. Math. Anal.* **33**, 286–314. (doi:10.1137/S0036141099360919)

24 Arnold, V. I., Afrajmovich, V. S., Ilyashenko, Yu. S. & Shilnikov, L. P. 1999 *Bifurcation theory and catastrophe theory*. Berlin, Germany: Springer.

25 Szmolyan, P. & Wechselberger, M. 2001 Canards in $\mathbb{R}^3$. *J. Differ. Equ.* **177**, 419–453. (doi:10.1006/jdeq.2001.4001)

26 Nene, N. R. & Zaikin, A. 2010 Gene regulatory network attractor selection and cell fate decision: insights into cancer multi-targeting. In *Proc. of Biosignal 2010, Berlin, Germany, 14–16 July 2010*. See http://www.ucl.ac.uk/~rmjbale/PAPERS_OWN/75_2010_Nene_Zaikin.pdf.